FERMILAB-Pub-97/109-E

Measurement of the Top Quark Pair Production Cross Section in $p\overline{p}$ Collisions

The DØ Collaboration*
Fermi National Accelerator Laboratory, Batavia, Illinois 60510
(April 22, 1997)

arXiv:hep-ex/9704015v1 25 Apr 1997

Abstract

We present a measurement of the $t\bar{t}$ production cross section in $p\bar{p}$ collisions at $\sqrt{s} = 1.8$ TeV by the DØ experiment at the Fermilab Tevatron. The measurement is based on data from an integrated luminosity of approximately 125 pb^{-1} accumulated during the 1992–1996 collider run. We observe 39 $t\bar{t}$ candidate events in the dilepton and lepton+jets decay channels with an expected background of 13.7 ± 2.2 events. For a top quark mass of 173.3 GeV/c^2, we measure the $t\bar{t}$ production cross section to be 5.5 ± 1.8 pb.

Typeset using REVTEX

*Authors listed on the following page.
Submitted to Physical Review Letters.

S. Abachi,[14] B. Abbott,[28] M. Abolins,[25] B.S. Acharya,[43] I. Adam,[12] D.L. Adams,[37] M. Adams,[17] S. Ahn,[14] H. Aihara,[22] G.A. Alves,[10] E. Amidi,[29] N. Amos,[24] E.W. Anderson,[19] R. Astur,[42] M.M. Baarmand,[42] A. Baden,[23] V. Balamurali,[32] J. Balderston,[16] B. Baldin,[14] S. Banerjee,[43] J. Bantly,[5] J.F. Bartlett,[14] K. Bazizi,[39] A. Belyaev,[26] S.B. Beri,[34] I. Bertram,[31] V.A. Bezzubov,[35] P.C. Bhat,[14] V. Bhatnagar,[34] M. Bhattacharjee,[13] N. Biswas,[32] G. Blazey,[30] S. Blessing,[15] P. Bloom,[7] A. Boehnlein,[14] N.I. Bojko,[35] F. Borcherding,[14] J. Borders,[39] C. Boswell,[9] A. Brandt,[14] R. Brock,[25] A. Bross,[14] D. Buchholz,[31] V.S. Burtovoi,[35] J.M. Butler,[3] W. Carvalho,[10] D. Casey,[39] Z. Casilum,[42] H. Castilla-Valdez,[11] D. Chakraborty,[42] S.-M. Chang,[29] S.V. Chekulaev,[35] L.-P. Chen,[22] W. Chen,[42] S. Choi,[41] S. Chopra,[24] B.C. Choudhary,[9] J.H. Christenson,[14] M. Chung,[17] D. Claes,[27] A.R. Clark,[22] W.G. Cobau,[23] J. Cochran,[9] W.E. Cooper,[14] C. Cretsinger,[39] D. Cullen-Vidal,[5] M.A.C. Cummings,[16] D. Cutts,[5] O.I. Dahl,[22] K. Davis,[2] K. De,[44] K. Del Signore,[24] M. Demarteau,[14] D. Denisov,[14] S.P. Denisov,[35] H.T. Diehl,[14] M. Diesburg,[14] G. Di Loreto,[25] P. Draper,[44] J. Drinkard,[8] Y. Ducros,[40] L.V. Dudko,[26] S.R. Dugad,[43] D. Edmunds,[25] J. Ellison,[9] V.D. Elvira,[42] R. Engelmann,[42] S. Eno,[23] G. Eppley,[37] P. Ermolov,[26] O.V. Eroshin,[35] V.N. Evdokimov,[35] T. Fahland,[8] M. Fatyga,[4] M.K. Fatyga,[39] J. Featherly,[4] S. Feher,[14] D. Fein,[2] T. Ferbel,[39] G. Finocchiaro,[42] H.E. Fisk,[14] Y. Fisyak,[7] E. Flattum,[14] G.E. Forden,[2] M. Fortner,[30] K.C. Frame,[25] S. Fuess,[14] E. Gallas,[44] A.N. Galyaev,[35] P. Gartung,[9] T.L. Geld,[25] R.J. Genik II,[25] K. Genser,[14] C.E. Gerber,[14] B. Gibbard,[4] S. Glenn,[7] B. Gobbi,[31] M. Goforth,[15] A. Goldschmidt,[22] B. Gómez,[1] G. Gómez,[23] P.I. Goncharov,[35] J.L. González Solís,[11] H. Gordon,[4] L.T. Goss,[45] A. Goussiou,[42] N. Graf,[4] P.D. Grannis,[42] D.R. Green,[14] J. Green,[30] H. Greenlee,[14] G. Grim,[7] S. Grinstein,[6] N. Grossman,[14] P. Grudberg,[22] S. Grünendahl,[39] G. Guglielmo,[33] J.A. Guida,[2] J.M. Guida,[5] A. Gupta,[43] S.N. Gurzhiev,[35] P. Gutierrez,[33] Y.E. Gutnikov,[35] N.J. Hadley,[23] H. Haggerty,[14] S. Hagopian,[15] V. Hagopian,[15] K.S. Hahn,[39] R.E. Hall,[8] S. Hansen,[14] J.M. Hauptman,[19] D. Hedin,[30] A.P. Heinson,[9] U. Heintz,[14] R. Hernández-Montoya,[11] T. Heuring,[15] R. Hirosky,[15] J.D. Hobbs,[14] B. Hoeneisen,[1,†] J.S. Hoftun,[5] F. Hsieh,[24] Ting Hu,[42] Tong Hu,[18] T. Huehn,[9] A.S. Ito,[14] E. James,[2] J. Jaques,[32] S.A. Jerger,[25] R. Jesik,[18] J.Z.-Y. Jiang,[42] T. Joffe-Minor,[31] K. Johns,[2] M. Johnson,[14] A. Jonckheere,[14] M. Jones,[16] H. Jöstlein,[14] S.Y. Jun,[31] C.K. Jung,[42] S. Kahn,[4] G. Kalbfleisch,[33] J.S. Kang,[20] R. Kehoe,[32] M.L. Kelly,[32] C.L. Kim,[20] S.K. Kim,[41] A. Klatchko,[15] B. Klima,[14] C. Klopfenstein,[7] V.I. Klyukhin,[35] V.I. Kochetkov,[35] J.M. Kohli,[34] D. Koltick,[36] A.V. Kostritskiy,[35] J. Kotcher,[4] A.V. Kotwal,[12] J. Kourlas,[28] A.V. Kozelov,[35] E.A. Kozlovski,[35] J. Krane,[27] M.R. Krishnaswamy,[43] S. Krzywdzinski,[14] S. Kunori,[23] S. Lami,[42] H. Lan,[14,*] R. Lander,[7] F. Landry,[25] G. Landsberg,[14] B. Lauer,[19] A. Leflat,[26] H. Li,[42] J. Li,[44] Q.Z. Li-Demarteau,[14] J.G.R. Lima,[38] D. Lincoln,[24] S.L. Linn,[15] J. Linnemann,[25] R. Lipton,[14] Q. Liu,[14,*] Y.C. Liu,[31] F. Lobkowicz,[39] S.C. Loken,[22] S. Lökös,[42] L. Lueking,[14] A.L. Lyon,[23] A.K.A. Maciel,[10] R.J. Madaras,[22] R. Madden,[15] L. Magaña-Mendoza,[11] S. Mani,[7] H.S. Mao,[14,*] R. Markeloff,[30] L. Markosky,[2] T. Marshall,[18] M.I. Martin,[14] K.M. Mauritz,[19] B. May,[31] A.A. Mayorov,[35] R. McCarthy,[42] J. McDonald,[15] T. McKibben,[17] J. McKinley,[25] T. McMahon,[33] H.L. Melanson,[14] M. Merkin,[26] K.W. Merritt,[14] H. Miettinen,[37] A. Mincer,[28] J.M. de Miranda,[10] C.S. Mishra,[14] N. Mokhov,[14] N.K. Mondal,[43] H.E. Montgomery,[14] P. Mooney,[1] H. da Motta,[10] C. Murphy,[17] F. Nang,[2] M. Narain,[14] V.S. Narasimham,[43] A. Narayanan,[2] H.A. Neal,[24] J.P. Negret,[1] P. Nemethy,[28] D. Nešić,[5]

M. Nicola,[10] D. Norman,[45] L. Oesch,[24] V. Oguri,[38] E. Oltman,[22] N. Oshima,[14] D. Owen,[25] P. Padley,[37] M. Pang,[19] A. Para,[14] Y.M. Park,[21] R. Partridge,[5] N. Parua,[43] M. Paterno,[39] J. Perkins,[44] M. Peters,[16] R. Piegaia,[6] H. Piekarz,[15] Y. Pischalnikov,[36] V.M. Podstavkov,[35] B.G. Pope,[25] H.B. Prosper,[15] S. Protopopescu,[4] D. Pušeljić,[22] J. Qian,[24] P.Z. Quintas,[14] R. Raja,[14] S. Rajagopalan,[4] O. Ramirez,[17] L. Rasmussen,[42] S. Reucroft,[29] M. Rijssenbeek,[42] T. Rockwell,[25] N.A. Roe,[22] P. Rubinov,[31] R. Ruchti,[32] J. Rutherfoord,[2] A. Sánchez-Hernández,[11] A. Santoro,[10] L. Sawyer,[44] R.D. Schamberger,[42] H. Schellman,[31] J. Sculli,[28] E. Shabalina,[26] C. Shaffer,[15] H.C. Shankar,[43] R.K. Shivpuri,[13] M. Shupe,[2] H. Singh,[9] J.B. Singh,[34] V. Sirotenko,[30] W. Smart,[14] A. Smith,[2] R.P. Smith,[14] R. Snihur,[31] G.R. Snow,[27] J. Snow,[33] S. Snyder,[4] J. Solomon,[17] P.M. Sood,[34] M. Sosebee,[44] N. Sotnikova,[26] M. Souza,[10] A.L. Spadafora,[22] R.W. Stephens,[44] M.L. Stevenson,[22] D. Stewart,[24] D.A. Stoianova,[35] D. Stoker,[8] M. Strauss,[33] K. Streets,[28] M. Strovink,[22] A. Sznajder,[10] P. Tamburello,[23] J. Tarazi,[8] M. Tartaglia,[14] T.L.T. Thomas,[31] J. Thompson,[23] T.G. Trippe,[22] P.M. Tuts,[12] N. Varelas,[25] E.W. Varnes,[22] D. Vititoe,[2] A.A. Volkov,[35] A.P. Vorobiev,[35] H.D. Wahl,[15] G. Wang,[15] J. Warchol,[32] G. Watts,[5] M. Wayne,[32] H. Weerts,[25] A. White,[44] J.T. White,[45] J.A. Wightman,[19] S. Willis,[30] S.J. Wimpenny,[9] J.V.D. Wirjawan,[45] J. Womersley,[14] E. Won,[39] D.R. Wood,[29] H. Xu,[5] R. Yamada,[14] P. Yamin,[4] C. Yanagisawa,[42] J. Yang,[28] T. Yasuda,[29] P. Yepes,[37] C. Yoshikawa,[16] S. Youssef,[15] J. Yu,[14] Y. Yu,[41] Q. Zhu,[28] Z.H. Zhu,[39] D. Zieminska,[18] A. Zieminski,[18] E.G. Zverev,[26] and A. Zylberstejn[40]

(DØ Collaboration)

[1] *Universidad de los Andes, Bogotá, Colombia*
[2] *University of Arizona, Tucson, Arizona 85721*
[3] *Boston University, Boston, Massachusetts 02215*
[4] *Brookhaven National Laboratory, Upton, New York 11973*
[5] *Brown University, Providence, Rhode Island 02912*
[6] *Universidad de Buenos Aires, Buenos Aires, Argentina*
[7] *University of California, Davis, California 95616*
[8] *University of California, Irvine, California 92697*
[9] *University of California, Riverside, California 92521*
[10] *LAFEX, Centro Brasileiro de Pesquisas Físicas, Rio de Janeiro, Brazil*
[11] *CINVESTAV, Mexico City, Mexico*
[12] *Columbia University, New York, New York 10027*
[13] *Delhi University, Delhi, India 110007*
[14] *Fermi National Accelerator Laboratory, Batavia, Illinois 60510*
[15] *Florida State University, Tallahassee, Florida 32306*
[16] *University of Hawaii, Honolulu, Hawaii 96822*
[17] *University of Illinois at Chicago, Chicago, Illinois 60607*
[18] *Indiana University, Bloomington, Indiana 47405*
[19] *Iowa State University, Ames, Iowa 50011*
[20] *Korea University, Seoul, Korea*
[21] *Kyungsung University, Pusan, Korea*
[22] *Lawrence Berkeley National Laboratory and University of California, Berkeley, California 94720*
[23] *University of Maryland, College Park, Maryland 20742*
[24] *University of Michigan, Ann Arbor, Michigan 48109*
[25] *Michigan State University, East Lansing, Michigan 48824*
[26] *Moscow State University, Moscow, Russia*
[27] *University of Nebraska, Lincoln, Nebraska 68588*
[28] *New York University, New York, New York 10003*
[29] *Northeastern University, Boston, Massachusetts 02115*
[30] *Northern Illinois University, DeKalb, Illinois 60115*
[31] *Northwestern University, Evanston, Illinois 60208*
[32] *University of Notre Dame, Notre Dame, Indiana 46556*
[33] *University of Oklahoma, Norman, Oklahoma 73019*
[34] *University of Panjab, Chandigarh 16-00-14, India*
[35] *Institute for High Energy Physics, 142-284 Protvino, Russia*
[36] *Purdue University, West Lafayette, Indiana 47907*
[37] *Rice University, Houston, Texas 77005*
[38] *Universidade Estadual do Rio de Janeiro, Brazil*
[39] *University of Rochester, Rochester, New York 14627*
[40] *CEA, DAPNIA/Service de Physique des Particules, CE-SACLAY, Gif-sur-Yvette, France*
[41] *Seoul National University, Seoul, Korea*
[42] *State University of New York, Stony Brook, New York 11794*
[43] *Tata Institute of Fundamental Research, Colaba, Mumbai 400005, India*
[44] *University of Texas, Arlington, Texas 76019*
[45] *Texas A&M University, College Station, Texas 77843*

The discovery [1] of the top quark in 1995 at the Fermilab Tevatron collider ended a long search following the 1977 discovery of the b quark [2] and represents another triumph of the Standard Model (SM). In the SM, the top quark completes the third fermion generation. A measurement of the top quark pair production cross section is of interest as a test of QCD predictions. A deviation from these predictions could indicate non-standard production or decay processes.

In $p\overline{p}$ collisions at $\sqrt{s} = 1.8$ TeV, top and anti-top quarks are predominantly pair produced through $q\overline{q}$ annihilation ($\approx$90%) or gluon fusion ($\approx$10%). In the SM, due to their large mass, they decay before they hadronize; nearly all ($\geq$99.8%) decay to a W boson and a b quark. The subsequent W decay determines the major signatures of $t\overline{t}$ decay. In the dilepton channel, both W bosons decay either to $e\nu$ or $\mu\nu$. The branching fraction for this channel is rather small (4/81), but it has the advantage of small backgrounds. In the lepton+jets channel, one W boson decays to $e\nu$ or $\mu\nu$ and the other hadronically. The branching fraction is 24/81. The dominant source of background for this channel is W+jets production.

In this Letter we report a measurement of the $t\overline{t}$ production cross section ($\sigma_{t\overline{t}}$) using the entire data sample (125$\pm$7 pb^{-1}) collected during the 1992–1996 collider run. This is more than twice the data described in our previous publication [1]. Different trigger conditions cause the integrated luminosity to vary from channel to channel. The analysis presented here is optimized to maximize the expected precision of the $t\overline{t}$ cross section measurement.

A detailed description of the DØ detector, trigger, and algorithms for reconstructing jets and missing transverse energy $\not\!\!E_T$ is found in Refs. [3] and [4]. The current electron and muon identification algorithms provide better rejection of backgrounds and increased efficiencies than those used in Ref. [4].

The signature of the dilepton channel consists of two isolated high p_T leptons, two or more jets, and large $\not\!\!E_T$. The selection criteria are summarized in Table I. Several additional cuts that remove specific backgrounds have been omitted from the table, but are noted below. In Table I, η is the pseudorapidity, H_T is the scalar sum of the E_T of all jets with $E_T \geq 15$ GeV, and $H_T^e = H_T + E_T$(leading electron). Three $e\mu$ events, one ee event, and one $\mu\mu$ event survive the selection criteria.

The signature of the lepton+jets channel consists of one isolated high p_T lepton, $\not\!\!E_T$ due to the neutrino, and several jets. In these events, jets are produced by the hadronization of two b quarks and the two quarks from W boson decay. Thus we expect to see four jets. However, due to gluon radiation and merging of jets, the number of detected jets may vary. After requiring an isolated high p_T lepton, $\not\!\!E_T$, and at least three jets, we expect 50 events from $t\overline{t}$ production (assuming top quark mass $m_t = 170$ GeV/c^2) but observe 550 events, due primarily to W+jets production. To enhance the relative contribution of events from top quark decays, we employ two techniques. One method, denoted ℓ+jets/μ, requires a jet to be associated with a tag muon as evidence of the semileptonic decay of a b quark. A requirement on the minimum separation between the muon and the reconstructed jet $\Delta\mathcal{R}_{\rm jet} = \sqrt{\Delta\eta^2 + \Delta\phi^2}$ defines this association. The other method, denoted ℓ+jets, is applied to events without tag muons. It exploits the difference in event shape and kinematics between $t\overline{t}$ and background. Selection criteria for both methods are described in Table I. Note that the requirements on event shape variables are less stringent for the ℓ+jets/μ analysis.

To select the optimal variables and their threshold values that yield the best precision for

TABLE I. Kinematic selection criteria for decay channels included in the cross section measurement. An event may populate only one channel. All energies are in GeV.

	dilepton	ℓ+jets	ℓ+jets/μ	$e\nu$
lepton p_T	> 15	> 20	> 20	> 20
	> 20 (ee)			
electron $\lvert\eta\rvert$	< 2.5	< 2.0	< 2.0	< 1.1
muon $\lvert\eta\rvert$	< 1.7	< 1.7	< 1.7	—
$\not\!\!E_T$	> 20 ($e\mu$)	> 25 (e)	> 20	> 50
	> 25 (ee)	> 20 (μ)		
jet E_T	> 20	> 15	> 20	> 30
jet $\lvert\eta\rvert$	< 2.5	< 2.0	< 2.0	< 2.0
# of jets	≥ 2	≥ 4	≥ 3	≥ 2
H_T^e	> 120(ee,$e\mu$)	—	—	—
H_T	> 100 ($\mu\mu$)	> 180	> 110	—
$\mathcal{A}$	—	> 0.065	> 0.040	—
E_T^L	—	> 60	—	—
η_W	—	< 2.0	—	—
tag muon	—	veto	$p_T > 4$	—
			$\Delta\mathcal{R}_{\rm jet} < 0.5$	
$M_T^{e\nu}$	—	—	—	>115

the measured cross section, we perform an optimization using a random grid search technique [5]. We use a Monte Carlo (MC) $t\bar{t}$ sample generated with $m_t = 170$ GeV/c^2 to compute the expected signal event yield for various cutoffs, while we determine the backgrounds using the methods described below. Variables that provide significant discrimination between $t\bar{t}$ events and backgrounds are H_T; the aplanarity $\mathcal{A}$ computed using W boson and jet momenta in the laboratory frame [6]; and E_T^L, the scalar sum of the lepton E_T and $\not\!\!E_T$. A requirement on the pseudorapidity η_W of the W boson which decays leptonically [7] is imposed in the ℓ+jets analysis to obtain better agreement between background control samples from data and the W+jets MC samples. In Fig. 1, we show plots of the two kinematic variables $\mathcal{A}$ and H_T, after imposing all cuts except those on the variables plotted, for our ℓ+jets data sample, $t\bar{t}$ MC and the two background sources: multijet and W+4 jets events. The cuts indicated by the dashed lines provide a good separation between the expected signal and backgrounds. The optimized selection criteria listed in Table I yield 9 e+jets, 10 μ+jets, 5 e+jets/μ, and 6 μ+jets/μ events.

We gain increased acceptance for $t\bar{t}$ production through a more inclusive channel, the $e\nu$ channel, which requires an isolated high E_T electron, $\not\!\!E_T > 50$ GeV, transverse mass of $e\nu$, $M_T^{e\nu} > 115$ GeV, and two or more jets with $E_T > 30$ GeV. The $e\nu$ channel contains top signal mainly from dileptons and e+jets top decays which fail the standard kinematic selection. Four events survive the $e\nu$ requirements listed in Table I.

For all channels, the number of $t\bar{t}$ events expected to pass the selection criteria is calculated for top quark masses between 140 and 200 GeV/c^2. Samples of $t\bar{t}$ decays to all

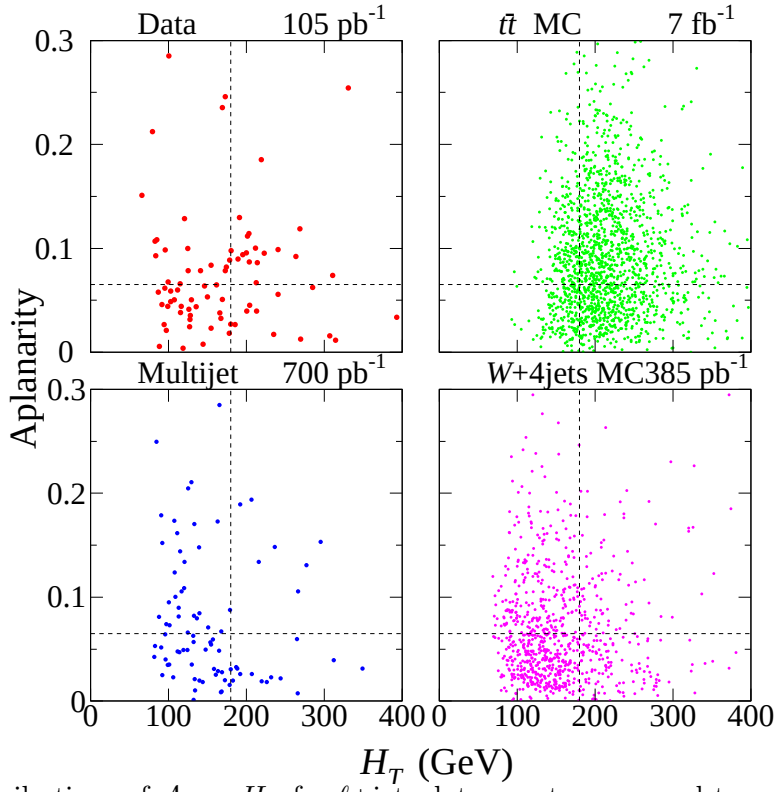

FIG. 1. Distributions of $\mathcal{A}$ vs. H_T for ℓ+jets data events compared to expectations for higher luminosity samples of $t\bar{t}$ (m_t = 170 GeV/c^2), multijet, and W+4jets backgrounds. The dashed lines represent the threshold values used for the selection.

TABLE II. Event yields

channel	events observed	background	expected signal m_t (GeV/c^2) 150	170	190
dilepton	5	1.4±0.4	5.9±1.0	4.1±0.7	2.6±0.5
ℓ+jets	19	8.7±1.7	18.3±6.3	14.1±3.1	9.2±1.4
ℓ+jets/μ	11	2.4±0.5	9.1±1.7	5.8±1.0	3.7±0.6
$e\nu$	4	1.2±0.4	2.5±0.8	1.7±0.5	1.1±0.3
total	39	13.7±2.2	35.9±8.8	25.7±4.6	16.6±2.4

possible final states are produced with the HERWIG event generator [8] and a GEANT model of the DØ detector [9]. We filter MC events according to the same criteria as used for data. Therefore, the acceptances include events with $W \to \tau\nu$ decays that pass the selection cuts. The acceptances computed from MC are refined by incorporating lepton selection efficiencies measured using $Z \to ee, \mu\mu$ data. Table II lists the expected number of signal events, computed using the $t\bar{t}$ production cross section of Ref. [10], for three top quark masses

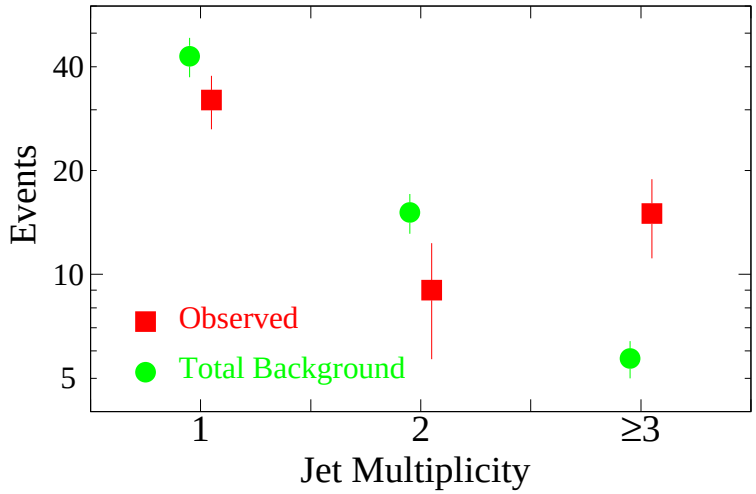

FIG. 2. Jet multiplicity spectrum of ℓ+jets/μ events before imposing event shape $(\mathcal{A}, H_T)$ criteria, compared to background estimates.

along with the number of observed events. The errors quoted include the uncertainty in the jet energy scale, differences between the HERWIG and ISAJET [11] event generators, lepton identification, and trigger efficiencies.

We distinguish between physics backgrounds, which have the same final states as the signal process, and instrumental backgrounds in which objects in the final state were misidentified. Instrumental backgrounds for all channels are estimated entirely from data, using control samples consisting of multijet events and the measured probability for misidentifying a jet as a lepton [4]. For the physics backgrounds discussed below, the distributions for W+jets background are modeled using the VECBOS event generator [12] which is interfaced to HERWIG to fragment the partons. The background estimates for all analyses are summarized in Table II.

Sources for physics backgrounds depend on the channel under consideration. The main physics backgrounds to the dilepton channels are Z boson, Drell-Yan, and vector boson pair production. These are estimated by MC simulations, and corrected for efficiencies measured in collider data. In the $e\mu$ channel, the signal to background ratio is ≈10:1, where about half of the total background is due to $Z \to \tau\tau$ events. In the $\mu\mu$ channel, Z decays are rejected by a kinematic fit to the $Z \to \mu\mu$ hypothesis. The $Z \to ee$ background is reduced by raising the cut on $\not\!\!E_T$ to 40 GeV for dielectron masses within 12 GeV of the Z mass. The dominant physics background process for the $e\nu$ channel is $W(\to e\nu)$+jets production and is strongly suppressed by the large transverse mass requirement. To estimate this background, we use the number of $W+\geq 2$ jets events observed in our data before the transverse mass cut and the rejection of the $M_T^{e\nu}$ cut determined using W+2 jets MC. Contributions to the uncertainty in the background include 12% for variations in the jet energy scale (15% for $e\nu$), 10% for uncertainties in the cross sections used for MC samples, 15% for modeling of H_T and H_T^e distributions in the MC, and typically 5% for multiple interactions. For the $\mu\mu$ channel there is an additional 10% uncertainty for the kinematic fit.

In the ℓ+jets channel, physics backgrounds arise mainly from W+jets production. We

estimate the W+jets background for events with four or more jets by extrapolating from a W+jets data sample at low jet multiplicities, assuming that the number of W+jets events falls exponentially with the number of jets in the event ($N_{\rm jets}$ scaling) [12]. We have checked our W+jets data sample at jet multiplicities between one and three, before event shape cuts ($\mathcal{A}, H_T$), and it supports this scaling law [4]. We then apply the survival probability for event shape cuts which is determined to be $9 \pm 1\%$ from W+4 jets MC. The uncertainty in the background estimate includes a 10% error on the validity of the $N_{\rm jets}$ scaling law (determined using Z+jets, γ+jets and multijet control samples), 5% for jet energy scale variations, and 15% for differences in event shape variables between background and MC W+ 2 jets and W+ 3 jets samples.

The principal source of background in the ℓ+jets/μ analysis is also W+jets production. We assume the heavy flavor content in W+jets events is the same as in multijet events [4]. The probability of tagging a jet in the absence of $t\bar{t}$ production is then determined by the fraction of jets in multijet events that are tagged. We parameterize the tagging rate as a function of jet E_T and η. By comparing the predicted and observed number of tags in several data samples with jet E_T thresholds varying from 20 to 85 GeV, we assign a systematic uncertainty of 10% to this procedure. We then apply this tagging rate to each jet in a background dominated sample satisfying all selection criteria in Table I except the b-tag requirement. For the μ+jets/μ final state, we reject $Z(\rightarrow \mu\mu)$+jets events, where one of the muons is counted as a tagging muon, by using a kinematic fit to the Z decay hypothesis. This residual background is estimated using a MC simulation. Figure 2 shows the jet multiplicity spectrum of ℓ+jets/μ events and the background estimates before event shape ($\mathcal{A}, H_T$) cuts. There is good agreement for 1 and 2 jet samples, while a clear excess is observed at 3 or more jets, indicative of $t\bar{t}$ production.

Overall, 39 events satisfy the selection criteria. We expect 13.7±2.2 events from background sources and 24.2±4.1 $t\bar{t}$ events, assuming $m_t = 173$ GeV/c^2 and the predicted cross section of Ref. [10]. The total acceptance for $t\bar{t}$ events varies between 2.8% and 4.9% for top quark masses between 150 and 190 GeV/c^2. Figure 3 shows the measured $t\bar{t}$ cross section versus top quark mass, compared to three theory calculations [10,13,14]. The error band accounts for statistical and systematic uncertainties, both in the backgrounds and acceptances, and takes account of the correlations among channels. The systematic uncertainty has a component due to m_t dependent variations between MC generators (gen) used to model top production, while all other fractional systematic uncertainties are m_t independent.

We quote $\sigma_{t\bar{t}}$ at our central value $m_t = 173.3$ GeV/c^2 [7]. Cross section measurements for the individual channels are consistent with each other; we measure 6.3 ± 3.3 pb from dilepton and $e\nu$, 4.1 ± 2.0 pb from ℓ+jets, and 8.2 ± 3.5 pb from ℓ+jets/μ events. Combining them gives $\sigma_{t\bar{t}} = 5.5 \pm 1.4(\text{stat}) \pm 0.9(\text{syst}) \pm 0.6(\text{gen})$ pb, in good agreement with the SM predictions. Adding the three uncertainties in quadrature, we measure the $t\bar{t}$ production cross section to be 5.5 ± 1.8 pb.

We thank the staffs at Fermilab and collaborating institutions for their contributions to this work, and acknowledge support from the Department of Energy and National Science Foundation (U.S.A.), Commissariat à L'Energie Atomique (France), State Committee for Science and Technology and Ministry for Atomic Energy (Russia), CNPq (Brazil), Departments of Atomic Energy and Science and Education (India), Colciencias (Colombia), CONACyT (Mexico), Ministry of Education and KOSEF (Korea), CONICET and UBACyT

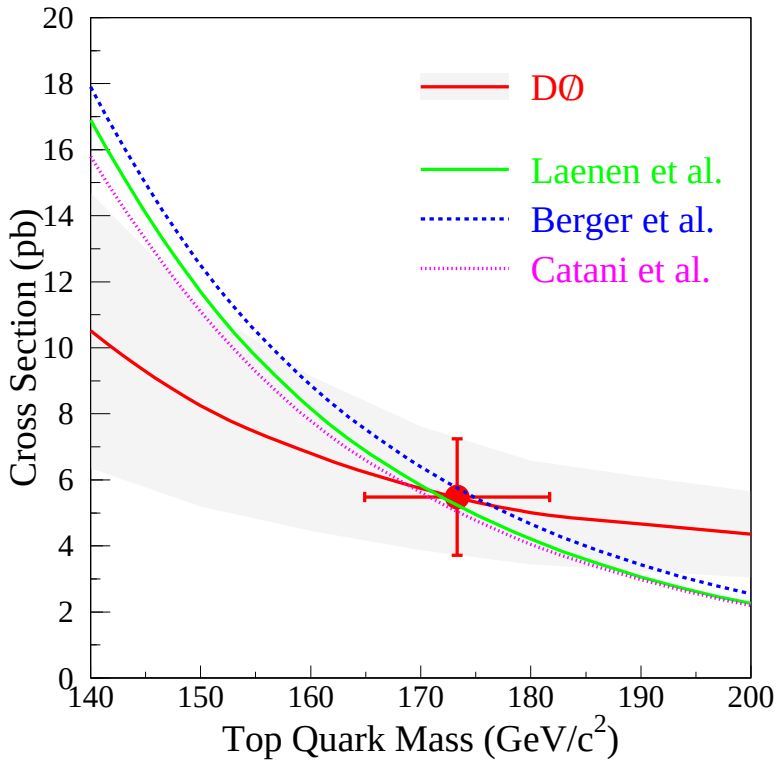

FIG. 3. Measured $t\bar{t}$ production cross section as a function of m_t (shaded band). The point with error bars is the cross section for the measured top quark mass at DØ. Three different theoretical estimates are also shown.

(Argentina), and the A.P. Sloan Foundation.

REFERENCES

* Visitor from IHEP, Beijing, China.

† Visitor from Universidad San Francisco de Quito, Quito, Ecuador.

[1] CDF Collaboration, F. Abe *et al.*, Phys. Rev. Lett. **74**, 2626 (1995); DØ Collaboration, S. Abachi *et al.*, Phys. Rev. Lett. **74**, 2632 (1995).

[2] S.W. Herb *et al.*, Phys. Rev. Lett. **39**, 252 (1977).

[3] DØ Collaboration, S. Abachi *et al.*, Nucl. Instrum. Methods **A338**, 185 (1994).

[4] DØ Collaboration, S. Abachi *et al.*, Phys. Rev. D**52**, 4877 (1995).

[5] N. Amos *et al.*, Proc. Intl. Conf. on Computing in High Energy Physics, Rio de Janeiro, Brazil, ed. R. Shellard, T. D. Nguyen. (World Scientific, Singapore, 1995).

[6] V. Barger, J. Ohnemus and R. J. N. Phillips, Phys. Rev. D **48**, 3953 (1993).

[7] DØ Collaboration, S. Abachi *et al.*, submitted to Phys. Rev. Lett. (1997); Fermilab-Pub-97/059-E; hep-ex/9703008.

[8] G. Marchesini *et al.*, Comp. Phys. Comm. **67**, 465, (1992).

[9] R. Brun and F. Carminati, CERN Program Library Long Writeup W5013, 1993 (unpublished).

[10] E. Laenen, J. Smith, and W. van Neerven, Phys. Lett. **B321**, 254 (1994).

[11] F. Paige and S. Protopopescu, BNL Report BNL38034, 1986 (unpublished), release 7.21.

[12] F. A. Berends, H. Kuijf, B. Tausk, and W. T. Giele, Nucl. Phys. B357, 32 (1991).

[13] E. Berger and H. Contopanagos, Phys. Lett. **B361**, 115 (1995) and Phys. Rev. D **54**, 3085 (1996).

[14] S. Catani, M.L. Mangano, P. Nason, and L. Trentadue, Phys. Lett. **B378**, 329 (1996).

	dilepton	ℓ+jets	ℓ+jets/μ	$e\nu$
lepton p_T	> 15	> 20	> 20	> 20
	> 20 (ee)			
electron $\lvert\eta\rvert$	< 2.5	< 2.0	< 2.0	< 1.1
muon $\lvert\eta\rvert$	< 1.7	< 1.7	< 1.7	—
$\not{E}_T$	> 20 $(e\mu)$	> 25 (e)	> 20	> 50
	> 25 (ee)	> 20 (μ)		
jet E_T	> 20	> 15	> 20	> 30
jet $\lvert\eta\rvert$	< 2.5	< 2.0	< 2.0	< 2.0
# of jets	≥ 2	≥ 4	≥ 3	≥ 2
H_T^e	$> 120(ee,e\mu)$	—	—	—
H_T	> 100 $(\mu\mu)$	> 180	> 110	—
$\mathcal{A}$	—	> 0.065	> 0.040	—
E_T^L	—	> 60	—	—
η_W	—	< 2.0	—	—
tag muon	—	veto	$p_T > 4$	—
			$\Delta\mathcal{R}_{\rm jet} < 0.5$	
$M_T^{e\nu}$	—	—	—	>115

channel	events observed	background	expected signal m_t (GeV/c^2) 150	170	190
dilepton	5	1.4±0.4	5.9±1.0	4.1±0.7	2.6±0.5
ℓ+jets	19	8.7±1.7	18.3±6.3	14.1±3.1	9.2±1.4
ℓ+jets/μ	11	2.4±0.5	9.1±1.7	5.8±1.0	3.7±0.6
$e\nu$	4	1.2±0.4	2.5±0.8	1.7±0.5	1.1±0.3
total	39	13.7±2.2	35.9±8.8	25.7±4.6	16.6±2.4